An Abrupt Decrease in the Late-Season Typhoon Activity over the Western North Pacific*

PANG-CHI HSU

Earth System Modeling Center, Nanjing International Academy of Meteorological Sciences, Nanjing University of Information Science and Technology, Nanjing, China, and International Pacific Research Center, University of Hawai'i at Mānoa, Honolulu, Hawaii

PAO-SHIN CHU

Department of Meteorology, School of Ocean and Earth Science and Technology, University of Hawai'i at Mānoa, Honolulu, Hawaii

HIROYUKI MURAKAMI

International Pacific Research Center, University of Hawai'i at Mānoa, Honolulu, Hawaii, and Meteorological Research Institute, Tsukuba, Japan

XIN ZHAO

Department of Meteorology, School of Ocean and Earth Science and Technology, University of Hawai'i at Mānoa, Honolulu, Hawaii

(Manuscript received 16 July 2013, in final form 18 February 2014)

ABSTRACT

In 1995 an abrupt shift in the late-season (October–December) typhoon activity over the western North Pacific (WNP) is detected by a Bayesian changepoint analysis. Interestingly, a similar change also occurs in the late-season sea surface temperature series over the western Pacific, eastern North Pacific, and portions of the Indian Ocean. All of the counts, lifespans, and accumulated cyclone energy of the late-season typhoons during the 1995–2011 epoch decreased significantly, compared with typhoons that occurred during the 1979–94 epoch. The negative vorticity anomaly is found to be the leading contributor to the genesis potential index (GPI) decrease over the southeastern sector of the WNP during 1995–2011. To elucidate the origin of the epochal change in the dynamic environmental conditions, a suite of sensitivity experiments is conducted based on the latest version of the Japan Meteorological Research Institute atmospheric general circulation model (MRI AGCM). The ensemble simulations suggest that the recent change to a La Niña–like state induces an unfavorable dynamic condition for typhoon genesis over the southeastern WNP. Warming in the Indian Ocean, however, contributes insignificantly to the circulation anomaly related to typhoon genesis over the southeastern WNP. The frequency of typhoon occurrence reveals a basinwide decrease over the WNP in the recent epoch, except for a small increase near Taiwan. An empirical statistical analysis shows that the basinwide decrease in the frequency of the typhoon occurrence is primarily attributed to a decrease in typhoon genesis, while the change in track is of less importance.

1. Introduction

Tropical cyclones (TCs) with maximum sustained winds ≥ 64 kt ($1\,\text{kt} \approx 0.51\,\text{m s}^{-1}$) are known as typhoons in the western North Pacific and are one of the most destructive natural disasters throughout the world. Based on the Regional Specialized Meteorological Center (RSMC) Tokyo–Typhoon Center records for 1979–2011 (Fig. 1), approximately 4.6 typhoons occurred during the

* Earth System Modeling Center Contribution Number 001.

Corresponding author address: Pang-Chi Hsu, College of Atmospheric Science, Nanjing University of Information Science and Technology, No. 219, Ningliu Road, Nanjing 210044, China.
E-mail: pangchi.hsu@gmail.com

DOI: 10.1175/JCLI-D-13-00417.1

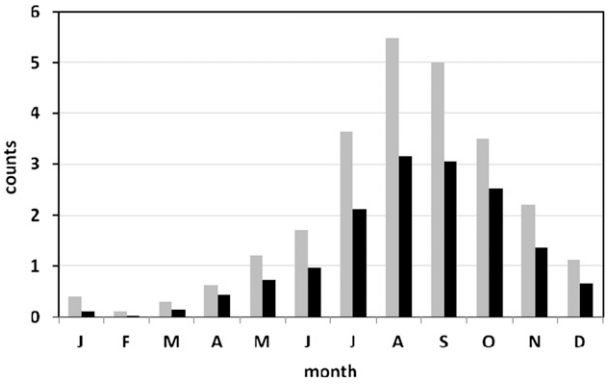

FIG. 1. Climatological monthly mean counts of the tropical cyclones with 10-min winds >30 kt (gray bars) and the typhoons (tropical cyclones with 10-min winds >56 kt, black bars) over the WNP (0°–60°N, 100°E–180°) for the period 1979–2011. Source: RSMC Tokyo.

late season [October–December (OND)], accounting for 30% of the annual typhoon numbers (15) over the western North Pacific (WNP). Although the actual number of typhoons is less in the late season than during the peak season [July–September (JAS)], a higher percentage of the late-season TCs develop into typhoons. About 67% (59%) of tropical cyclones intensify into typhoons during the late (peak) season (Fig. 1).

In recent years, a number of catastrophic typhoons occurred in the late season. For example, category 5 Supertyphoon Bopha (2012), generated in late November, killed at least 1146 people, caused $1.04 billion in damage in the Philippines, and became the costliest Philippine typhoon on record. Supertyphoon Megi (2010), which formed in mid-October, also caused enormous damage ($735.9 million) to the Philippines, Taiwan, and China. More recently, an exceptionally powerful typhoon (Haiyan) devastated the central Philippine in early November 2013. It is the deadliest Philippine typhoon in modern history, killing more than 5000 people in that country. It is also worth mentioning that the largest TC ever recorded in the WNP, Supertyphoon Tip (1979), was also a late-season typhoon. While late-season typhoons may impose great impacts on society and individual lives, their long-term variability and associated mechanisms have not been adequately addressed.

In the North Atlantic, an increase in the annual number and destructiveness of intense hurricanes has been found in the past few years (e.g., Goldenberg et al. 2001; Emanuel 2005; Webster et al. 2005; Kossin et al. 2007; Elsner et al. 2008). The causes of this recent increase, however, are still being debated. Some studies suggest that anthropogenic warming leads to an increase in the intensity of hurricanes (Webster et al. 2005; Holland and Webster 2007). Other studies have attributed the change to natural variability (Landsea 2005; Chan 2006, 2008). Compared to the North Atlantic, recent trends in typhoon or TC intensity in the WNP have proven less obvious (Kossin et al. 2007). Numerous studies found that the WNP typhoon counts and characteristics (frequency, intensity, track, and relationship with the SST) of TCs experienced multidecadal variability (Matsuura et al. 2003; Ho et al. 2004; Wu et al. 2005; Chan 2008; Liu and Chan 2008; Tu et al. 2009; Yeh et al. 2010; Tu et al. 2011; Yokoi and Takayabu 2013; Liu and Chan 2013). The active and inactive phases of TC activity on decadal time scales can be largely attributed to decadal changes in the large-scale atmospheric and oceanic environments.

Sea surface temperature (SST) variability shows a significant linkage with the variations of TC activity. In the Atlantic, the upward trend in SST is highly correlated with the increase in the intensity of hurricane activity (Webster et al. 2005; Emanuel 2005). Although the variability of typhoons is negatively correlated with the local SST (Chan 2006), the SST variations in both the tropical eastern Pacific (i.e., El Niño–Southern Oscillation) and Indian Ocean have been reported to play an important role in the interannual variability of TCs (e.g., Wang and Chan 2002; Camargo et al. 2007; Zhan et al. 2011; Du et al. 2011). Recently, Jin et al. (2013) showed that the off-equatorial SST warming over the central Pacific provides a favorable environment for TC motion toward East Asia during the central Pacific El Niño events. Therefore, SST changes even in the remote region such as the central Pacific will influence large-scale circulation and TC activity over the WNP.

Previous studies, up to the present, have focused on either the variability of annual typhoon counts or TC activity during the peak season. Very little attention has been paid to the late season activity, although the typhoons in this season have considerable impact. In this study, we will examine whether there are significant changes in typhoons over the WNP during the late season, and the mechanisms responsible for any changes. In particular, we will examine how local and remote SST changes on decadal time scales modulate typhoon genesis over the WNP. These issues will be addressed by using the following methodologies: a statistical changepoint analysis, sensitivity experiments using an atmospheric general circulation model (AGCM), and a newly developed empirical statistical analysis for typhoon frequency.

In section 2, we introduce the data, analysis methods, and model experiments. In section 3, the timing of an abrupt change in the late-season typhoon activity and SST is detected and discussed. Then the typhoon-related features before and after the regime shift are examined. In section 4, the dynamical and thermodynamic factors responsible for the abrupt changes in typhoon genesis are discussed. Moreover, the role of regional SST changes on

the changes in typhoon genesis over the WNP is clarified, based on the results of the numerical model experiments. Section 5 quantitatively examines the relative contributions of the typhoon genesis, tracks, and nonlinearity to the epochal changes in the frequency of typhoon occurrence. A summary and discussion are provided in section 6.

2. Data, model, and methodology

a. Data

The tropical cyclone best-track data over the WNP (0°–60°N, 100°E–180°), including the South China Sea (SCS) basin, are obtained from the RSMC Tokyo–Typhoon Center, Japan Meteorological Agency (RSMC 2012). The dataset consists of TC information, such as the location, intensity (maximum 10-min sustained wind), and minimum surface pressure at 6-h intervals from 1951 to present. The timing of extratropical transitions is also included in this dataset. To ensure data reliability, the data for the recent 33-yr satellite period of 1979–2011 are used. Considering the possible inconsistencies among best-track datasets (Wu et al. 2006; Kamahori et al. 2006), best-track data from the Joint Typhoon Warning Center (JTWC; JTWC 2012) for the same analysis period are also used to confirm the results of the RSMC Tokyo dataset.

Typhoons are commonly defined as TCs with sustained surface wind speed of over 64 kt. It is noted that the JTWC dataset records a 1-min sustained wind speed, while the RSMC Tokyo dataset uses a 10-min sustained wind speed. As indicated by Simiu and Scanlon (1978), the strength of the 10-min sustained wind is statistically 88% of the 1-min sustained wind. Thus we reduce the threshold to 56-kt 10-min wind speed for detecting typhoon cases in the RSMC Tokyo dataset. This approach has been applied to the International Best Track Archive for Climate Stewardship (IBTrACS) project and used operationally (Knapp et al. 2010). Because of this conversion, the typhoon strength here is slightly weaker than that from the RSMC Tokyo official classification, which is based on a threshold of 64-kt 10-min sustained wind speed.

Typhoon positions are counted for each 2.5° × 2.5° grid box within the WNP domain at 6-h intervals. The typhoon frequency is defined as the total count for each grid box. The location of the typhoon genesis is defined as the first position at which the maximum wind speed exceeds 30 (34) kt in the RSMC Tokyo (JTWC) dataset. The definition of typhoon lifespan is the period from typhoon genesis to the timing of extratropical transition or of tropical cyclone dissipation.

Several dynamical and thermodynamic variables are used to describe the large-scale environmental conditions. These variables are as follows: monthly-mean sea level pressure, zonal and meridional wind components, vertical pressure velocity, air temperature, and specific humidity from the European Centre for Medium-Range Weather Forecasts (ECMWF) Interim Re-Analysis (ERA-Interim; Simmons et al. 2007); monthly-mean SST from the Met Office Hadley Centre Sea Ice and Sea Surface Temperature dataset, version1 (HadISST1; Rayner et al. 2003); and monthly-mean precipitation from the Global Precipitation Climatology Project (GPCP; Adler et al. 2003). The horizontal resolutions of the ERA-Interim, HadISST1, and GPCP datasets are 1.5°, 1°, and 2.5° latitude–longitude, respectively.

b. Numerical model experiments

To understand how the regional SST anomalies modulate the critical circulation conditions that affect the epochal changes in typhoon activity, we use an AGCM forced by different boundary conditions. The model used in this study is adapted from the Meteorological Research Institute AGCM, version 3.2 (MRI AGCM3.2) at T_L95 spectral truncation horizontal resolution (~200 km). This is the newest version of the MRI AGCM with an upgraded cumulus parameterization, which is referred to as the Yoshimura cumulus scheme. Using the new cumulus parameterization, the MRI AGCM3.2 substantially improves the simulations of large-scale circulations and precipitation (Mizuta et al. 2012), as well as the distribution and intensity of tropical cyclones (Murakami et al. 2012) from the older version of the MRI AGCM3.1. Details of model physics and performance are documented in Mizuta et al. (2012).

c. Statistical changepoint analysis

A Bayesian paradigm under the one changepoint hypothesis is used to objectively detect when a regime shift in TC activity occurs (Chu and Zhao 2004; Tu et al. 2009). This approach is briefly summarized by the following features: 1) the annual or seasonal number of tropical cyclones is modeled by a Poisson process where the Poisson intensity is codified by its conjugate gamma distribution, and 2) a hierarchical (i.e., structural layers) approach involving three layers—data, parameters, and hypothesis—is formulated to determine the posterior probability of the shift in time. The Bayesian analysis provides the probability information of changepoints rather than a deterministic estimate of the changepoint location. This is an advantage over the deterministic approach because the uncertainty inherent in statistical inferences is quantitatively expressed in the probability statement. Expanding from the analytical single changepoint analysis, Zhao and Chu (2010) developed an algorithm to analyze the inference for detecting multiple abrupt shifts in an extreme event count series. Readers may refer to Zhao and Chu (2010) and Chu and Zhao (2011) for the statistical hypothesis and formula of

Bayesian inference using statistical simulations with Monte Carlo methods.

In addition to typhoons, it is also of interest in this study to investigate whether there is an abrupt shift in the SST time series. Because temperature data usually follow a Gaussian distribution rather than a Poisson process, we revised the Poisson-gamma model by assuming that the mean and variance of the distribution change with time. The conjugate prior for the mean is a Gaussian and the conjugate prior for the variance is an inverted gamma distribution (e.g., Gill 2002). Otherwise the entire structure of the Bayesian inference for abrupt changes in SST is very similar to the typhoon series.

d. *An empirical statistical analysis for the typhoon frequency*

The distribution of typhoon genesis and preferable tracks may both exert influences on the variability of typhoon passage frequency. A new approach, proposed by Yokoi and Takayabu (2013) and Murakami et al. (2013), is applied to assess the relative importance of the typhoon genesis and track anomalies in a given period with respect to the climatology. Because a relatively larger number of typhoon samples help to prevent sampling errors, as suggested by Yokoi and Takayabu (2013), the analysis is performed with $5^\circ \times 5^\circ$ resolution.

The climatological average (denoted by an overbar) of typhoon frequency in a specific $5^\circ \times 5^\circ$ grid cell A can be written as

$$\overline{f}(A) = \iint_C \overline{g}(A_0)\overline{t}(A, A_0)\, dA_0, \tag{1}$$

where $g(A_0)$ is the frequency of typhoon genesis in a grid cell A_0, $t(A, A_0)$ is the probability that a typhoon generated in the grid cell A_0 travels to the grid cell A, and C is the entire domain of WNP over which the integration is performed.

The typhoon frequency anomalies (denoted by Δ) for a given period, relative to the climatological average, in a grid cell A is computed as

$$\begin{aligned}\Delta f(A) = &\iint_C \Delta g(A_0)\overline{t}(A, A_0)\, dA_0 \\ &+ \iint_C \overline{g}(A_0)\Delta t(A, A_0)\, dA_0 \\ &+ \iint_C \Delta g(A_0)\Delta t(A, A_0)\, dA_0. \end{aligned}\tag{2}$$

The first term on the right-hand side of Eq. (2) indicates how the changes in typhoon genesis contributes to the frequency of typhoon occurrence under the condition that the typhoon track is unchanged. The second term represents the contribution from the typhoon track anomalies. The third term is the nonlinear process related to both the typhoon genesis and track changes.

e. *Nonparametric tests for trends and epochal differences*

Tests of statistical significance are usually performed using a Student's t test, which assumes that two random variables are both characterized by Gaussian distributions. Because of the relatively small sample size in our 33-yr analysis, it is not guaranteed that the samples follow a Gaussian distribution. Thus, instead of using a t test, we opt to use the nonparametric rank-based Mann–Kendall test (Mann 1945; Kendall 1975) and the Wilcoxon–Mann–Whitney test (Wilcoxon 1945; Mann and Whitney 1947). The former is applied to estimate the significance of a trend and the latter to assess the difference in location (i.e., mean) between the two epochs (e.g., Chu 2002).

3. Abrupt changes in typhoon activity and SST

Figure 2a compares the time series of typhoon (TY) counts in OND over the WNP for the period 1979–2011 that were derived from the RSMC Tokyo and the JTWC datasets. The two time series are highly consistent with a correlation coefficient of 0.94. A decrease in the typhoon counts over the last 33 years is evident. The decreasing trends are robust in the two datasets. Both of them show a slope of around $-0.1\ \mathrm{yr}^{-1}$, which exceeds the 95% confidence level based on the Mann–Kendall test. Because the typhoon data show a very high consistency, we will only delineate the results using the RSMC Tokyo dataset in the analysis that follows.

Figure 2a also shows that the number of late-season typhoons range from 3 to 10 during the 1980s, and drops to below 5 (or even to only one or none) since the late 1990s. The periods of high and low typhoon counts seem to be separated by a sharp transition. To objectively detect the occurrence of any abrupt decrease in typhoon counts, we applied the Bayesian changepoint analysis, which estimates the posterior probabilities of each observation as a potential changepoint. The analysis result indicates an outstanding posterior probability of a shift in 1995 (Fig. 2b), implying that it is more likely that a change would occur in a new epoch with 1995 as the first year.

As shown in Fig. 2a, the average number of the late-season typhoon is 5.94 during 1979–94 (epoch 1 or E1), but is significantly reduced to 3.24 during 1995–2011 (epoch 2 or E2). This abrupt drop in the typhoon counts is statistically significant (Table 1). To examine if the

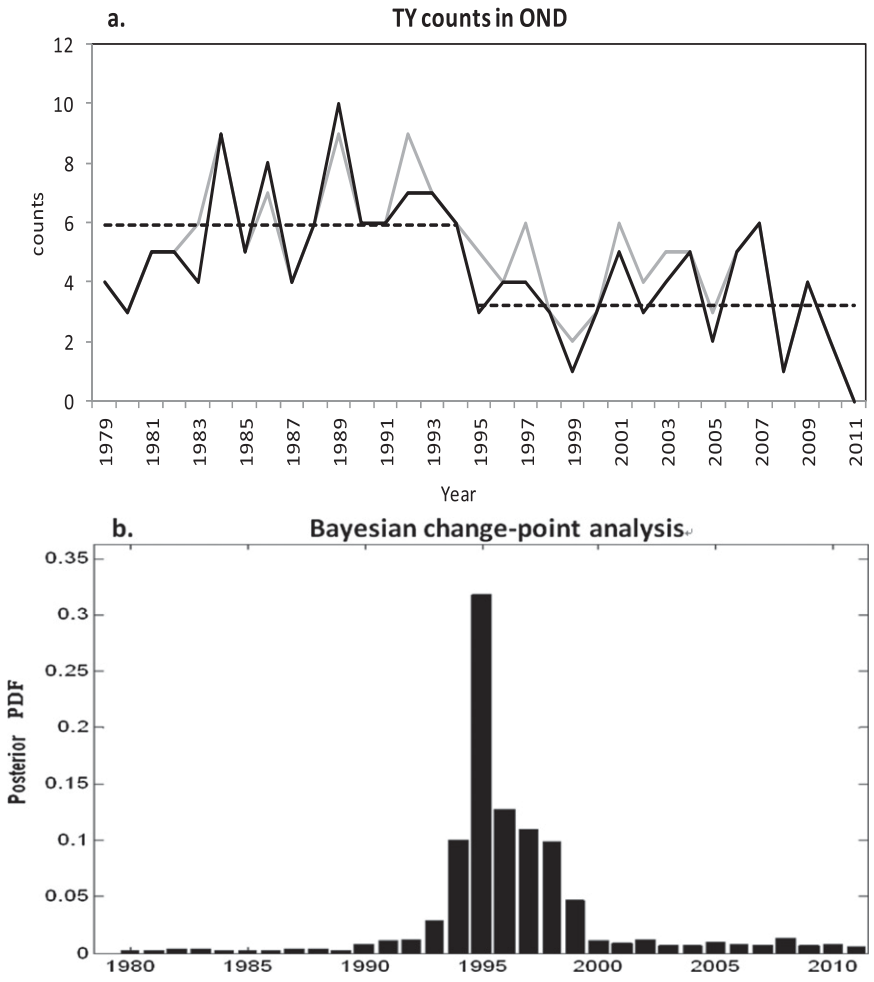

FIG. 2. (a) Time series of late-season (OND) typhoon counts in the WNP from 1979 to 2011. Black and gray lines illustrate the results from the RSMC Tokyo and the JTWC datasets, respectively. Dashed lines denote the means for the periods 1979–94 and 1995–2011, respectively. (b) The posterior probability mass function of the changepoint as a function of time (year). Source: RSMC Tokyo.

decrease in the late-season typhoon counts occurs during a specific month in the OND season, the number of typhoons from individual months is calculated. It turns out that the typhoon counts in all three late-season months (October, November, and December) decrease significantly in the recent epoch. The typhoon counts are nearly reduced in half from the previous peak epoch to the recent inactive epoch (Table 1). In addition to the remarkable difference in the number of typhoon geneses, the lifespans of the typhoons also experience a significant epochal change. The duration of a typhoon is on average about 5–8 days in the early epoch. In the more recent decade, late-season typhoons tend to be shorter-lived (about 3–6 days). As a result, the late-season accumulated cyclone energy (ACE; Bell et al. 2000), which takes into account the number, strength, and duration of all of the typhoons observed during OND over the WNP, largely decreases in 1995–2011. With regard to changes in lifespan and ACE of typhoons, the most significant drops occur in November (Table 1). Although the regime shift of late-season typhoon activity is evident, no changepoint is detected for the typhoon counts in peak season and individual months (August and September) during 1979–2011.

In addition to the typhoon change, it is worth analyzing whether the regime shift is also shown in other TC intensity categories. Here the tropical cyclone systems are classified into five different categorizes based on the 1-min sustained surface wind speed. TCs include all the systems attaining wind speed of over 34 kt. A tropical storm (TS) has wind speeds between 34 and 47 kt, while a severe TS has wind speed between 48 and 63 kt.

TABLE 1. Seasonal and monthly means of the late-season typhoon counts, lifespans and ACE for the early epoch (1979–94, E1) and recent epoch (1995–2011, E2), and the differences between the two epochs (E2 − E1). The *p* values in italics indicate that the epochal change is statistically significant at the 5% level based on the nonparametric Wilcoxon–Mann–Whitney rank-sum test.

	E1 (1979–94)	E2 (1995–2011)	E2 − E1	*p* value
TY count (number)				
OND	5.94	3.24	−2.70	*0.0002*
October	3.13	1.94	−1.19	*0.0163*
November	1.88	0.88	−1.00	*0.0062*
December	0.94	0.41	−0.53	*0.041*
TY lifespan (days)				
OND	6.61	4.37	−2.24	*0.0039*
October	7.80	6.18	−1.62	0.1195
November	7.11	3.64	−3.47	*0.0112*
December	4.92	3.28	−1.64	0.1056
TY ACE ($10^3\,m^2\,s^{-2}$)				
OND	32.69	21.20	−11.49	*0.0029*
October	40.66	31.50	−9.16	0.1552
November	36.82	17.36	−19.46	*0.0024*
December	20.58	14.73	−5.85	0.0843

Typhoons are categorized into two groups, categories 1–3 and categories 4 and 5, according to the Saffir–Simpson hurricane scale. Specifically, the first group has wind speeds between 64 and 112 kt and the second group has wind speeds greater than 113 kt.

As shown in Table 2, the average number of total late-season TCs per year is around 6.9 based on the RSMC Tokyo dataset. About 67% of the TCs may intensify to typhoon category, while a smaller portion (~33%) of the total TCs remains weaker than typhoon intensity (TS/severe TS). It is interesting to note that the weaker TCs did not show a statistically significant change on decadal time scales (i.e., a moderately large *p* value). Both the moderately intense (category 1–3) and extremely intense (category 4 and 5) TCs experienced a significant decrease from the earlier to the recent epochs with a much smaller *p* value. Because the typhoon-intensity systems dominate the late-season TCs (67%), the total TC counts also reveal a significant decrease in the recent decade (Table 2). The results derived from the JTWC dataset (not shown) are similar to those in the RSMC Tokyo dataset.

The abrupt change in the WNP typhoon counts may be linked to the tropical SST variability that influences the oceanic and atmospheric conditions for typhoon genesis. To examine if there are any decadal shifts of the late-season SST over the period of 1979–2011, we applied the changepoint analysis to the OND-averaged SST in each 5° × 5° point. The temporal and spatial patterns of the SST changes are shown in Fig. 3. A regime shift in the mid-1990s prevails over the tropical oceans, particularly in the western Pacific, eastern North Pacific, eastern South Pacific between the equator and 10°S, and some portions of the Indian Ocean. In the meantime, limited areas with regime shifts in the 1980s and 2000s are observed in the southwestern Indian Ocean and subtropical southeastern Pacific (south of 15°S). In the equatorial central-eastern Pacific, however, no significant changepoint could be identified. In section 4b, we will discuss in detail how the decadal shift of tropical SST affects the late-season typhoon activity over the WNP.

The epochal changes in the spatial distributions of typhoon genesis and frequency of occurrence are displayed in Fig. 4. The Asian monsoon trough, which is usually characterized by low-level cyclonic circulations, largely determines the genesis of tropical cyclones over the WNP (McBride 1995; Harr and Chan 2005; Molinari and Vollaro 2013). The monsoon trough retreats southward during the late season and the main genesis regions accordingly shift equatorward (Molinari and Vollaro 2013). Along with the decadal changes in the monsoon circulation, both the number and locations of the typhoon genesis undergo significant regime shifts. The low-level cyclonic circulation between 130° and 160°E is more enhanced in the early epoch than in the recent epoch (Figs. 4a,b). The weakened cyclonic circulation (or an anticyclonic anomaly) appears to lead to

TABLE 2. As in Table 1, but for the counts of late-season tropical cyclones with different intensity categories (cat). Time periods are defined as 79–11 for 1979–2011, 79–94 for 1979–94, and 95–11 for 1995–2011.

TC category	33 yr (79–11)	E1 (79–94)	E2 (95–11)	E2 − E1	*p* value
Total TC	6.87	8.25	5.48	−2.77	*0.0012*
TS	0.81	0.5	1.12	0.62	0.1037
Severe TS	1.47	1.81	1.12	−0.69	0.1037
Cat 1–3	3.7	4.81	2.59	−2.22	*0.000 25*
Cat 4 and 5	0.89	1.13	0.65	−0.48	*0.0331*

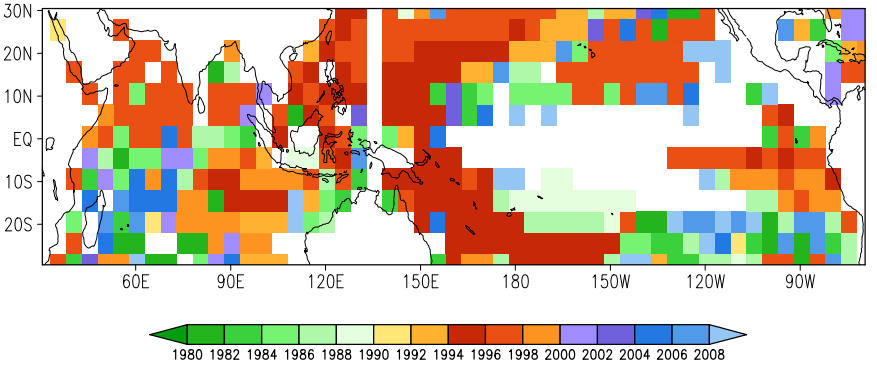

FIG. 3. Changepoint analysis of late-season SST during 1979–2011. Shading indicates when (year) the maximum probability of regime shift occurs, if the SST exists at a changepoint during the 33-yr time series, in each 5° × 5° point. Blank areas denote no significant changepoints.

a significant typhoon genesis decrease in the regions south of 17.5°N over the WNP and the SCS throughout the period 1995–2011 (Fig. 4b). A slight increase in typhoon genesis can also be found in a few patches of the subtropical regions (Fig. 4c). In the following section, we will investigate the possible mechanisms responsible for the changes in typhoon genesis.

The frequency of typhoon occurrence also shows significant decreases over most of the WNP basin, with the exception of a small increase in the typhoon frequency that appears near Taiwan in the recent epoch (Fig. 4f). The decreased typhoon genesis (Fig. 4c) may be one of the major contributors to the significant decreases in the typhoon frequency in the recent epoch (Fig. 4f). Another factor possibly affecting the typhoon frequency change may be typhoon track changes. In section 5, the effects of both typhoon genesis and tracks upon the epochal changes in the frequency of typhoon occurrence will be examined quantitatively.

4. Physical mechanisms for changes in typhoon genesis

a. Large-scale environmental conditions

It is known that the genesis of a tropical cyclone depends on large-scale atmospheric and oceanic conditions (e.g., Gray 1979). Figure 5 shows the epochal differences (E2 minus E1) within the large-scale environmental conditions that are associated with the abrupt changes in late-season typhoon genesis. Compared to conditions in the early epoch, an extensive banana-shaped warming region is observed over the western Pacific in the recent epoch (Fig. 5a). A smaller area of cooling (warming) occurs over the eastern Pacific (Indian Ocean). In a gross sense, the anomalous SST patterns mimic a La Niña condition. The shift of SST pattern in the mid to late 1990s has been identified by other studies (Burgman et al. 2008; Chikamoto et al. 2012). The warm (cold) SST anomaly associated with a La Niña–like state induces an anomalous low-level convergence (divergence) and a low (high) pressure anomaly over the tropical western (eastern) Pacific, suggesting a strengthening of the Walker circulation (Figs. 5e,f). The low-level easterly anomaly in the equatorial western Pacific associated with the anomalous Walker circulation may actually enhance the anticyclonic vorticity over the tropical WNP (Fig. 5b). Along with the anomalous downward motion in the tropical central-eastern Pacific (Fig. 5c), drying (Fig. 5g) and convective cooling (Fig. 5h) anomalies from the atmosphere induce an unfavorable condition for the development of tropical disturbances over the southeastern WNP (0°–17.5°N, 135°E–180°), where typhoon genesis decreases significantly in the recent decade (Fig. 4c). Moreover, the two leading effects, enhanced vertical wind shear and strengthened subtropical high, responsible for the low annual tropical cyclone numbers in 1998–2011 (Liu and Chan 2013) also exert their influences on the abrupt decrease in the late-season typhoon genesis for the period 1995–2011 (Figs. 5d and f).

The results of Fig. 5 suggest that the epochal changes in several dynamical and thermodynamic parameters may all be critical to the significant decrease in typhoon genesis during the late season in the recent epoch. To quantitatively identify the key factors, we examine the tropical cyclone genesis potential index (GPI). A modified version of the GPI (Murakami and Wang 2010) in which the vertical motion effect is incorporated into the original GPI formula (Emanuel and Nolan 2004) is used here:

$$\mathrm{GPI} = |10^5\eta|^{3/2}\left(\frac{\mathrm{RH}}{50}\right)^3\left(\frac{V_{\mathrm{pot}}}{70}\right)^3 \times (1+0.1V_s)^{-2}\left(\frac{-\omega+0.1}{0.1}\right), \qquad (3)$$

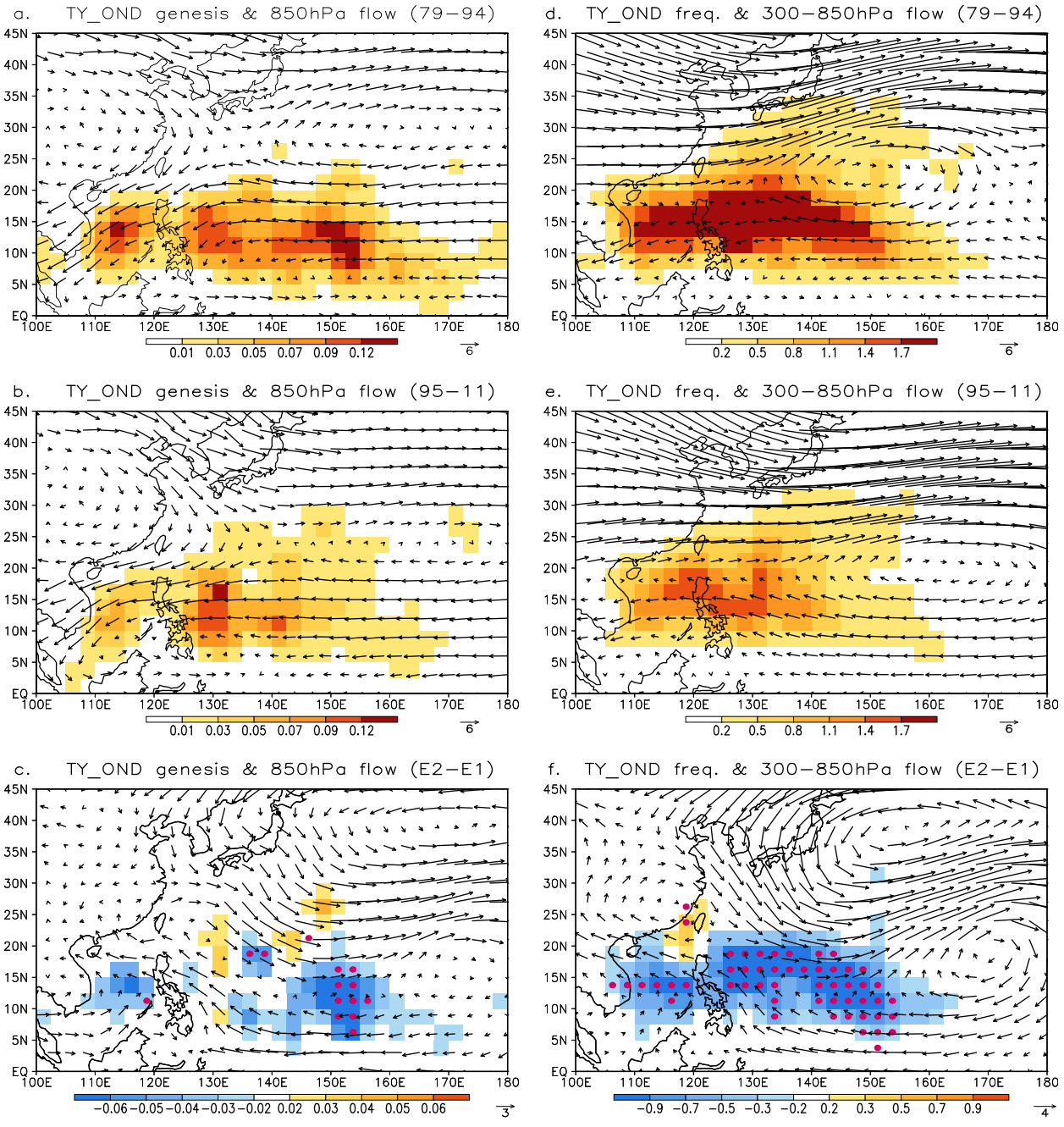

FIG. 4. The frequency of typhoon genesis derived from the RSMC Tokyo (shading, number per season) and 850-hPa wind field (vectors, m s^{-1}) during OND for the periods of (a) 1979–94 and (b) 1995–2011, and (c) their difference (1995–2011 minus 1979–94). (d)–(f) As in (a)–(c), but for the frequency of typhoon occurrence (shading) and the mass-weighted 300–850-hPa steering flow (vectors). The red dots in (c) and (f) mark the regions where the difference in typhoon genesis frequency between two epochs is statistically significant at the 5% level.

where η is the absolute vorticity (s^{-1}) at 850 hPa, RH is the relative humidity (%) at 700 hPa, $V_{\rm pot}$ is the maximum tropical cyclone potential intensity (PI; m s^{-1}), V_s is the magnitude of the vertical wind shear (m s^{-1}) between 850 and 200 hPa, and ω is the vertical pressure velocity (Pa s^{-1}) at 500 hPa. The definition of PI is based on work by Emanuel (1995) but modified by Bister and Emanuel (1998) as follows:

$$V_{\rm pot}^2 = \frac{C_k}{C_D}\frac{T_s}{T_0}(\mathrm{CAPE}^* - \mathrm{CAPE}^b), \qquad (4)$$

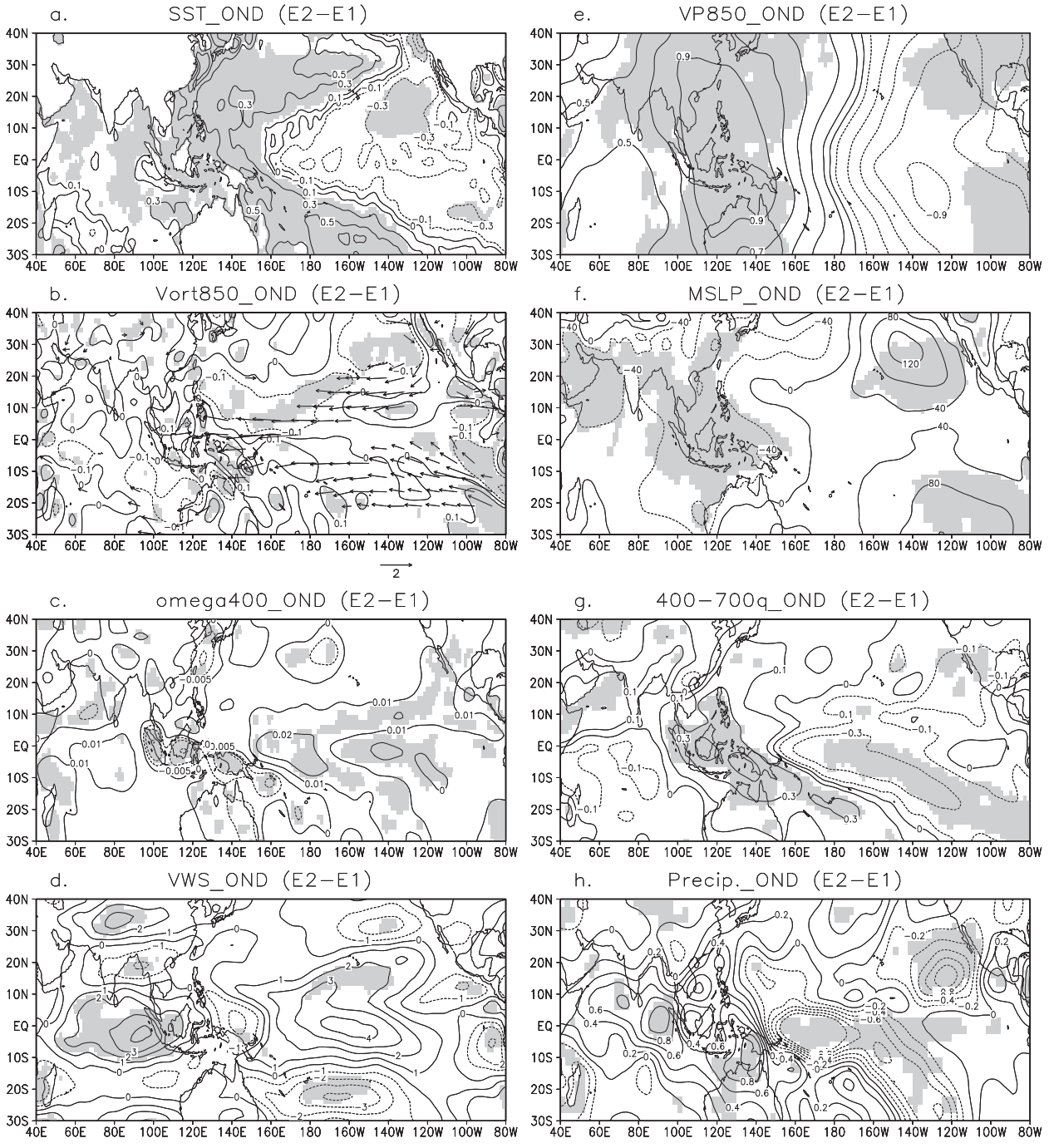

FIG. 5. Epochal changes in the large-scale environment during OND (1995–2011 minus 1979–94) for (a) SST (K), (b) 850-hPa vorticity ($10^{-5}\,s^{-1}$) and wind fields ($m\,s^{-1}$), (c) ω ($Pa\,s^{-1}$), (d) vertical wind shear ($m\,s^{-1}$), (e) velocity potential ($10^{6}\,m^{2}\,s^{-1}$), (f) mean sea level pressure (Pa), (g) 400–700-hPa averaged humidity ($10^{-3}\,kg\,kg^{-1}$), and (h) precipitation ($mm\,day^{-1}$). Shading marks regions where the difference between two epochs is statistically significant at the 5% level.

where C_k is the exchange coefficient for enthalpy, C_D is the drag coefficient, T_s is the SST (K), and T_0 is the mean outflow temperature (K). The quantity CAPE* is the value of the convective available potential energy (CAPE) with reference to environmental sounding, and $CAPE^b$ is that of the boundary layer air.

Figure 6 displays the total epochal change in the GPI during the late season (Fig. 6a), as well as the GPI

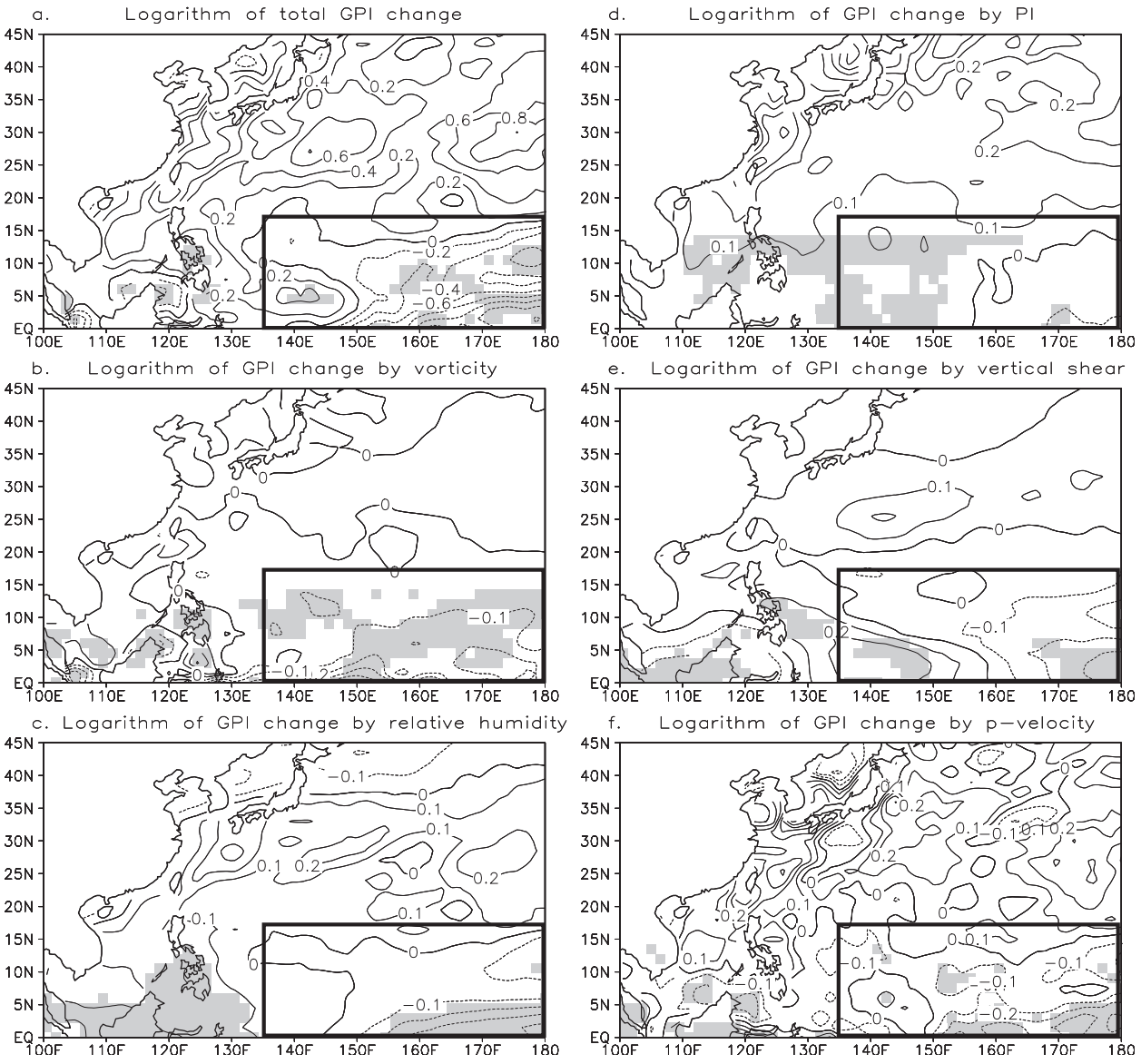

FIG. 6. As in Fig. 5, but for (a) the difference in GPI between the two epochs, and for GPI changes induced by individual terms: (b) vorticity, (c) RH, (d) maximum PI, (e) vertical shear, and (f) ω. The box indicates the region where typhoons decrease largely from the earlier to recent epochs.

changes obtained by varying each individual GPI element (i.e., variational GPI; Figs. 6b–f). By taking the logarithm in Eq. (3), the sum of the five variational GPI changes on the right-hand side is identical to the total GPI change. The negative anomalies of GPI and typhoon genesis both appear over the southeastern part of WNP (0°–17.5°N, 135°E–180°), although their maximum centers are not exactly collocated (Figs. 6a and 4c). Consistent with the results in Fig. 5, the anticyclonic vorticity (Fig. 6b), decreased humidity (Fig. 6c), enhanced vertical shear (Fig. 6e), and descending motion (Fig. 6f) together produce an unfavorable environment for typhoon genesis over the southeastern WNP during the recent epoch (1995–2011). This suggests that these dynamical variations (e.g., low-level vorticity, vertical wind shear, and vertical motion) play an essential role in causing the typhoons inactivity in the recent epoch, similar to the findings of Liu and Chan (2013). Among the dynamical effects, a negative vorticity anomaly of about 44% contributes to the negative GPI over the decreased typhoon genesis region (Table 3). Contributions from humidity, vertical wind shear, and vertical motion are comparable, accounting for 20%–24% of the total GPI change. The PI associated with warmer SST in

TABLE 3. Epochal changes in the total GPI and each budget term (i.e., varying vorticity, relative humidity, maximum potential intensity, vertical wind shear, and ω) over the region 0°–17.5°N, 135°E–180° where the typhoon genesis decreases significantly. The fractional contributions of each individual factor to the GPI anomaly are shown in parentheses.

Area average	GPI	Vorticity	RH	PI	V_s	ω
Value (contribution)	−0.25 (100%)	−0.11 (44%)	−0.06 (24%)	0.03 (−12%)	−0.05 (20%)	−0.06 (24%)

the tropical WNP contributes negatively to the decrease in the typhoon genesis (Fig. 6d). The change in PI appears to be minor (12%) compared to the GPI variation (Table 3). Our results showing the small but negative correlation between SST-related PI and typhoon genesis over the WNP are consistent with the findings in Chan (2009). Chan (2009) suggested that, in the WNP, the climate of intense TCs is unlikely to be controlled by thermodynamic factors.

The epochal change in the GPI indicates a high consistency with the decreased typhoon genesis in the southeastern WNP, as discussed above. In contrast to this, an out-of-phase relationship between the GPI and the typhoon genesis change is found over the SCS (Figs. 4c and 6a). This suggests that the decrease in late-season typhoon counts in the SCS could not be caused directly by the large-scale environmental changes in recent decades. However, the mechanisms responsible for this SCS typhoon genesis change are not the main focus of this study. Here, we briefly touch on a few of the possibilities. Apart from the conditions on a planetary scale, the activity of synoptic-scale disturbances (Takayabu and Nitta 1993), from which the typhoon may generate and grow, could be a factor. It is found that the 3–10-day synoptic-scale disturbances tend to weaken over the SCS in the late season of 1995–2011 (not shown). Another possible factor resulting in changes to the SCS typhoon genesis is related to the activity of cold surges during boreal winters. Previous studies (Chang et al. 2005; Lin and Lee 2011) indicated that the northeasterly cold-surge flows might lead to the intensification of convective disturbances in the SCS. In the recent epoch, the northeasterly flows associated with cold surge activity are reduced (not shown), suggesting a lower possibility for much cyclogenesis and development over the SCS.

b. *Role of regional SST changes*

Although the warming in the western Pacific contributes negatively to the typhoon genesis change through the local thermodynamic process (a positive PI anomaly in Table 3), the SST anomaly associated with a La Niña–like pattern could induce significant dynamical controls on the typhoon genesis change. In addition to the SST anomaly in the Pacific, the SST anomaly in the Indian Ocean can also affect TC frequency in the WNP by modulating the monsoon circulation and the equatorial Kelvin wave activity (Zhan et al. 2011; Du et al. 2011). To further elucidate how the SST over different basins may exert dynamical control over the typhoon genesis in the WNP, a suite of AGCM experiments is carried out.

The lower boundary conditions for the MRI AGCM are illustrated in Fig. 7. In the control experiment (EXP_CNTL), the global OND-mean SST in the early epoch (1979–94) is used (Fig. 7a). To examine the impacts of the tropical SST anomaly in the recent epoch, the differences in the SST between the two epochs (E2 minus E1), as shown in Fig. 7b, are added to the SST field in the EXP_CNTL. The experiment is then forced with the global SST in the control run and the eastern Pacific cooling (blue area in Fig. 7b), together with the western Pacific warming (red area in Fig. 7b), and finally the weaker warming in the Indian Ocean (yellow area in Fig. 7b). This experiment (EXP_EP+WP+IO) is designed to confirm if the changes to large-scale circulation and GPI are related to these tropical SST anomalies. Three additional individual experiments are conducted and forced with the SST in the control run along with SST anomalies in each of the three different basins (eastern Pacific, western Pacific, and Indian Ocean) separately in order to discuss the relative roles of local and remote SST anomalies to the changes in typhoon genesis over the WNP. The three experiments are referred to as EXP_EP, EXP_WP, and EXP_IO, respectively. To test more carefully if the eastern Pacific SST anomaly is essential to the decadal change in WNP typhoon, another sensitivity experiment excluding the eastern Pacific SST is performed by utilizing the SST anomalies over the western Pacific and Indian Ocean; this is named EXP_WP+IO.

To increase the robustness of simulated results, we conduct the ensemble simulations by using different initial conditions. To simulate the late-season conditions, we adopted 1 November in five random years as the initial condition for five ensemble members. The solar radiation at the top of the atmosphere is fixed at that existing on 1 November. All of the simulations are integrated for a period of 10 years after an initial spinup of 6 months. The simulated results shown here are averages of five ensemble runs for each experiment.

The GPI changes induced by all of the tropical SST anomalies (EXP_EP+WP+IO minus EXP_CNTL)

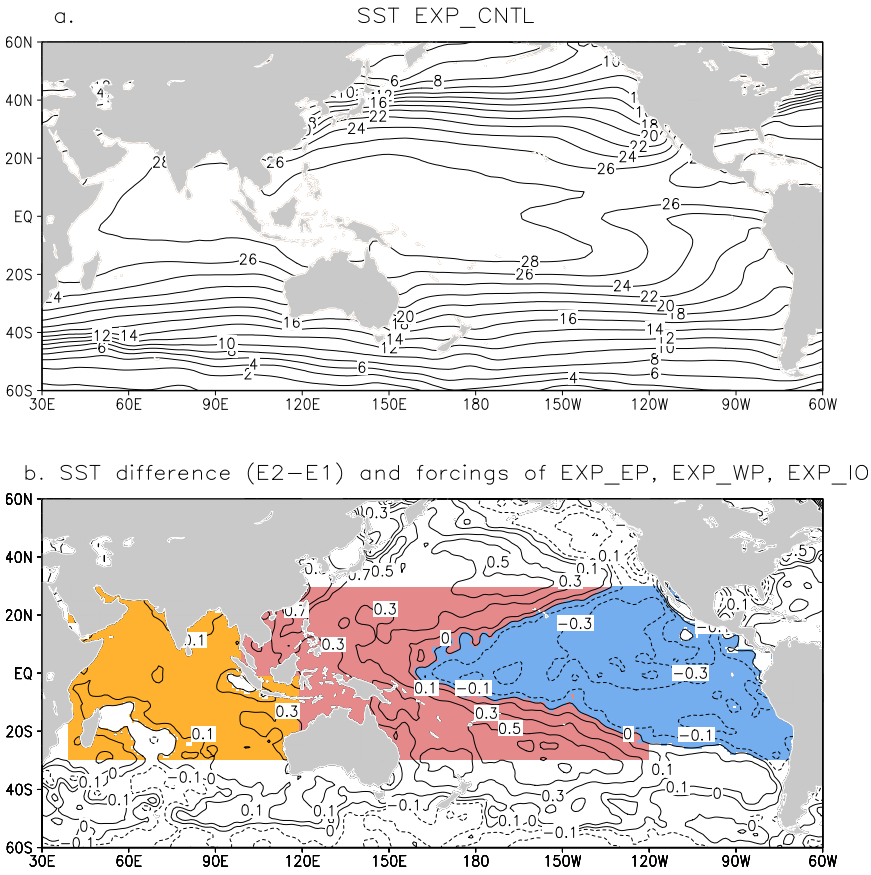

FIG. 7. (a) SSTs for the EXP_CNTL (°C). (b) Tropical SST anomalies (E2 minus E1, °C) that are added onto the SST in the EXP_CNTL to force the AGCM in the various experiments (blue for the EXP_EP, red for the EXP_WP, yellow for the EXP_IO, red and yellow for the EXP_WP+IO, and blue, red, and yellow together for the EXP_EP+WP+IO).

resemble observations, with a negative anomaly in the southeastern sector of the WNP and a positive anomaly in the western Pacific and the SCS (Figs. 8a and 6a). The negative (positive) GPI is consistent with the anticyclonic (cyclonic) anomaly over the tropical WNP (Fig. 8f). These results suggest that the epochal changes in the tropical SST over the Pacific basin and Indian Ocean together may account for the GPI changes via modulating the circulation over the WNP.

Now the question arises as to which ocean basin is more important in the simulated GPI changes. The western Pacific warming in the recent epoch plays a leading role in affecting the variations of GPI (Fig. 8b) as well as circulation (Fig. 8g), based on the comparisons between the EXP_WP, EXP_EP, and EXP_IO simulations. The highest temperature of a horseshoe-shaped warming occurs to the west of 130°E (Fig. 7b), which induces a local Walker circulation over the WNP. The west–east contrast of the GPI in Fig. 8b is associated with the low-level cyclonic anomaly in the ascending branch to the west of 130°E, and the anticyclonic anomaly in the descending branch in the southeastern sector of the WNP (Fig. 8g), where the typhoon genesis and GPI are reduced.

The recent cooling in the eastern Pacific plays a secondary role in causing the unfavorable environment for cyclogenesis in the southeastern part of the WNP. The difference between EXP_EP and EXP_CNTL indicates a small negative GPI and minor anticyclonic anomaly in the southeastern sector of the WNP (Figs. 8c,h). This change is not as significant as that in the EXP_WP (Figs. 8b,g). To confirm the small contribution from the eastern Pacific cooling, the EXP_WP+IO is further analyzed. Without the effect of SST cooling over the eastern Pacific, the negative GPI anomaly and a huge anticyclonic circulation to the east of 140°E responsible for the reduced typhoon counts can be seen in Figs. 8e and 8j. In comparison, the inclusion of eastern Pacific cooling together with the warming over the western Pacific and Indian Ocean (EXP_EP+WP+IO) displays a pattern similar to that in the EXP_WP+IO (Figs. 8a,f versus Figs. 8e,j). These results suggest that the eastern Pacific SST anomaly plays a minor role in

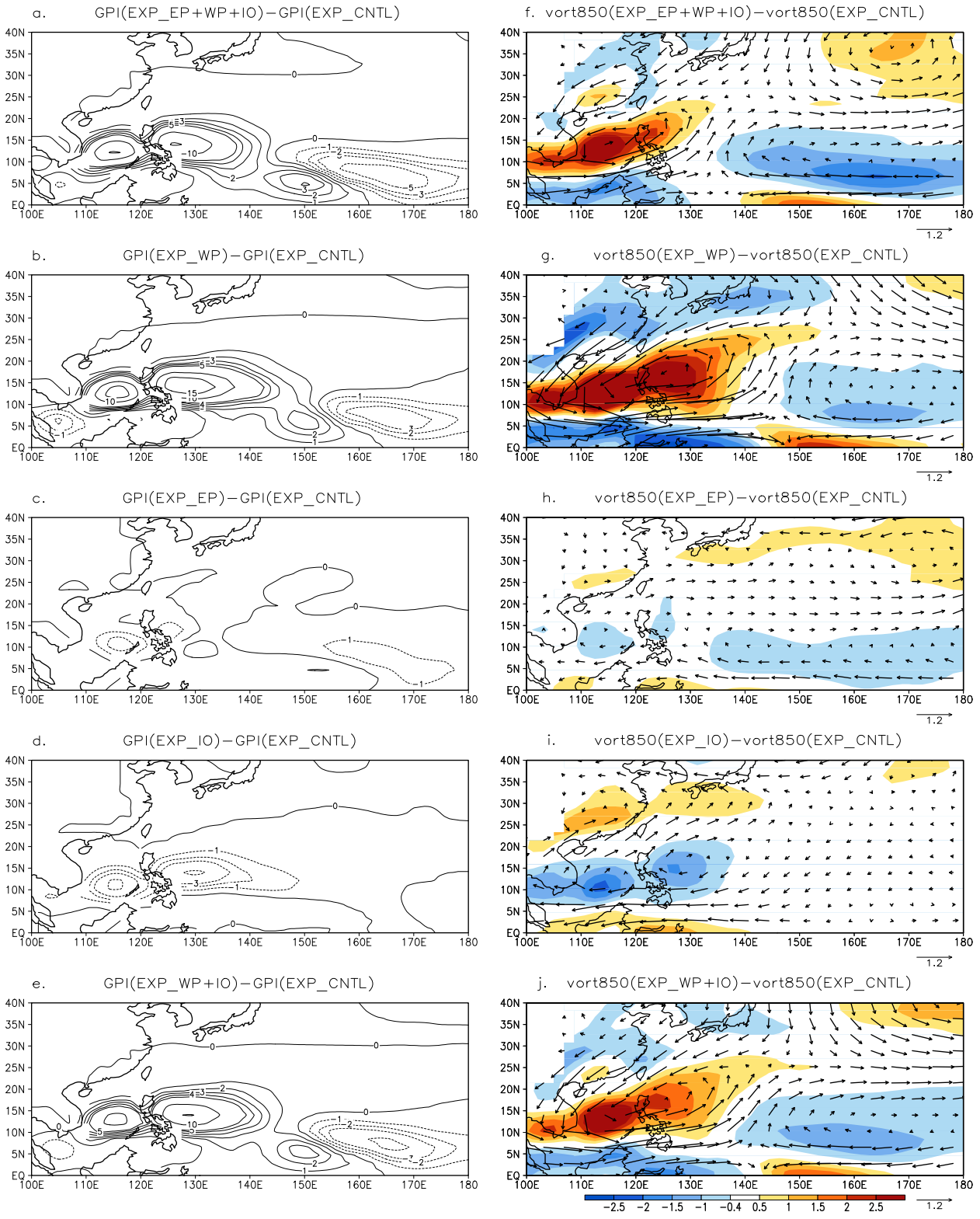

FIG. 8. Ensemble results of the GPI change simulated by (a) EXP_EP+WP+IO, (b) EXP_WP, (c) EXP_EP, (d) EXP_IO, and (e) EXP_WP+IO relative to the EXP_CNTL. (f)–(j) As in (a)–(e), but for the changes in 850-hPa vorticity (shading, $10^{-6}\,s^{-1}$) and wind field (vectors, $m\,s^{-1}$).

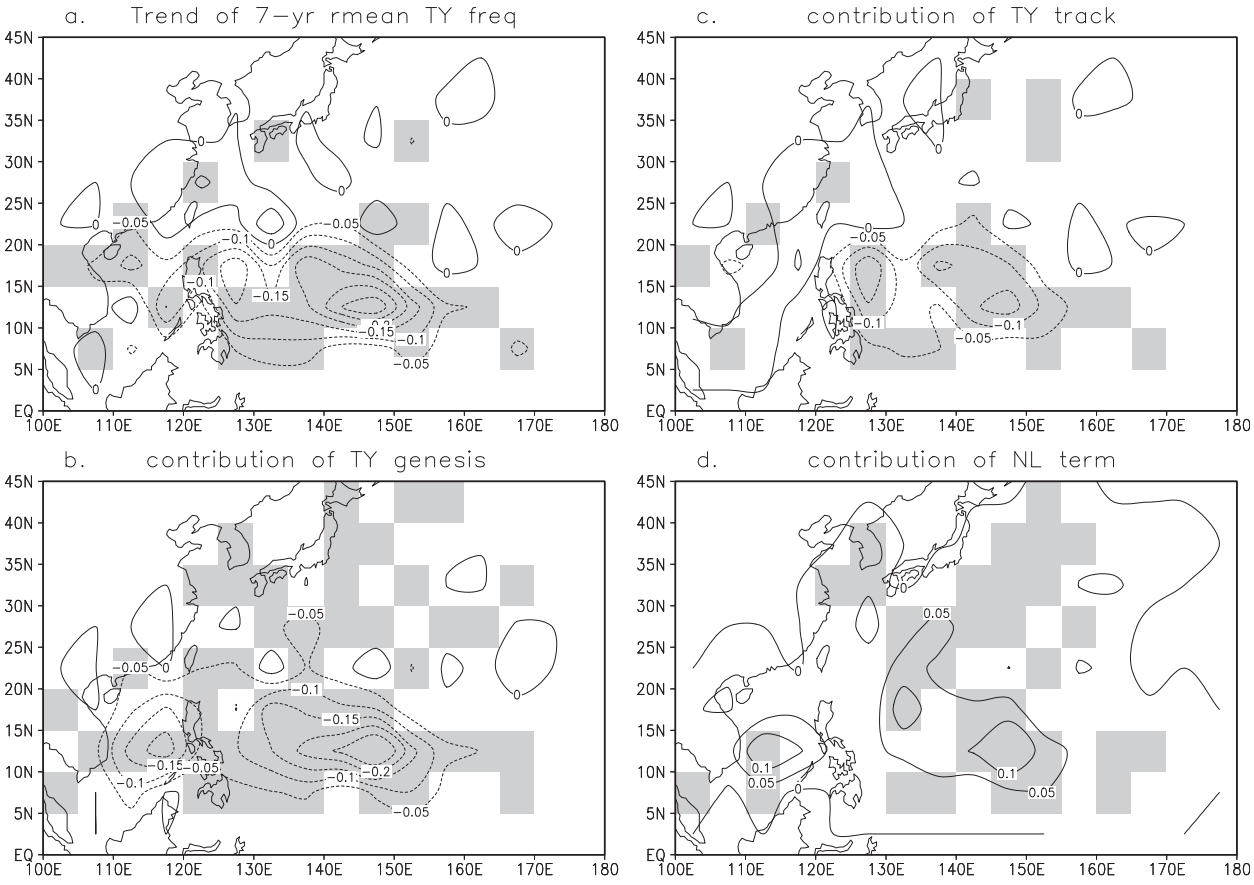

FIG. 9. (a) Linear trends in the frequency of typhoon occurrence in OND over the period of 1979–2011, and contributions of (b) genesis, (c) track, and (d) nonlinear effects. Shading indicates that the trend is statistically significant at the 5% level.

the decreased typhoon counts over the WNP in the recent epoch.

In the EXP_IO simulation, the Indian Ocean warming produces a negative GPI associated with an anomalous anticyclone in the WNP (Figs. 8d,i). However, the effect of the Indian Ocean warming in the recent epoch is confined to the west of 140°E (Fig. 8i) and is thus inconsistent with the observed changes in GPI and circulation (Figs. 6a,b). This limited influence is probably owing to the relatively weak warming of the Indian Ocean (0.1–0.3 K) in the recent epoch (Fig. 7b).

In summary, the atmospheric response to the La Niña–type SST anomaly in the recent decade is unfavorable for late-season typhoon genesis in the southeastern sector of the WNP. The contribution of the Indian Ocean warming to the typhoon genesis decrease is negligible, relative to the western Pacific warming and eastern Pacific cooling.

5. Reasons for changes in typhoon frequency

Following the passage frequency analysis methods proposed by Yokoi and Takayabu (2013) and Murakami et al. (2013), the relative importance of the typhoon genesis, track effect, and their covariance to the decadal change in typhoon frequency is examined. As suggested by Yokoi and Takayabu (2013), the anomalies in 7-yr moving periods were applied to obtain the interdecadal variability of the typhoon frequency and to infer its associated mechanisms.

Figure 9 shows the trends in the typhoon frequency along with three contributory terms on interdecadal time scales, based on the total analysis [Eq. (2)]. Consistent with the differences in the typhoon frequency between the two epochs (Fig. 4f), a large and significant decreasing trend in typhoon frequency over the tropical WNP–SCS basin as well as a weak increasing trend near Taiwan are observed (Fig. 9a). The decompositions of the typhoon frequency analysis suggest that the decrease in the typhoon frequency results mainly from the effect of lower typhoon genesis in the more recent periods (Fig. 9b). The contribution of the typhoon genesis effect is almost double when compared to the other two terms—track and nonlinear effects. Although the track effect is minor, it indicates a positive contribution to

both the decrease in the typhoon frequency over the tropical basins and the increase in the typhoon frequency near Taiwan (Fig. 9c). This result suggests that recent typhoons tend to spend a shorter period of time remaining in the tropical WNP, but are more likely to propagate into the Taiwan area. Interestingly, Tu et al. (2009) noted a northward shift in the typhoon track and an increase in typhoon frequency near Taiwan and the East China Sea since 2000. The nonlinearity of both the typhoon genesis and the track changes shows a negative contribution to the decreased typhoon frequency in the recent epoch (Fig. 9d).

6. Summary and discussion

There are around 6.9 TCs occurring in late season detected using the RSMC Tokyo dataset. About 67% of the TCs (i.e., 4.6) may intensify into typhoon intensity with a 10-min wind speed greater than 56 kt. Although these late-season typhoons have caused catastrophic damages to the Philippines and to other Asian countries in recent years, their long-term variabilities and associated mechanisms have not received much attention. Based on the Bayesian changepoint analysis, we find an abrupt shift in the late-season typhoon counts occurring in 1995. Typhoon numbers, durations, and the ACE reveal statistically significant declines in the recent epoch (1995–2011) compared with those in the previous epoch (1979–94). Contrast to the intense typhoons, the weaker tropical storms (TSs) did not show any significant changes between the two decades (Table 2). We also note a similar change in the late-season SST series over the western Pacific, eastern North Pacific, and portions of the Indian Ocean. The abrupt shift of WNP typhoon counts may be associated with the tropical SST variability that modulates atmospheric and oceanic conditions for typhoon genesis.

The spatial distribution of the typhoon genesis shows a basinwide decrease over the WNP and the SCS. Only a small increase in typhoon genesis could be noted in the subtropical WNP between 15° and 30°N. The largest decreases in the typhoon genesis appear in the southeastern sector of the WNP, where the GPI shows significant decreases, indicating that the epochal change in the late-season typhoon genesis might indeed be controlled by large-scale environmental conditions. Dynamical effects such as vorticity, vertical pressure velocity, and vertical wind shear play key roles in the recent decreases in typhoon genesis over the WNP (Fig. 6, Table 3), consistent with the findings in Liu and Chan (2013). A suite of AGCM experiments prescribed by the SST anomalies in various basins suggests that the La Niña–type SST anomaly causes circulation that is unfavorable for typhoon genesis over the WNP. The larger warming in the western Pacific induces a local Walker circulation with a descending (ascending) anomaly in the central (western) Pacific (Fig. 8g). Moreover, the cooling in the eastern Pacific enhances the anticyclonic anomaly over the southeastern WNP (Fig. 8h). The weak warming anomaly in the Indian Ocean exhibits an insignificant impact on the change in typhoon genesis in the southeastern WNP. The Indian Ocean warming-induced anticyclonic anomaly is confined to the western Pacific (west of 140°E) in the simulations (Fig. 8i).

The frequency of typhoon occurrence also reveals a basinwide decrease over the WNP for the period of 1995–2011 (with the exception of increased typhoon frequency in the vicinity of Taiwan). Both the changes in typhoon genesis and preferred track may influence this typhoon frequency variability. Empirical statistical analyses for typhoon frequency are applied to quantitatively examine the effects of typhoon genesis and track change on the decreases in typhoon frequency in recent decades (1995–2011). The results of the total analysis reveal that the substantial decrease in the likelihood of the typhoon frequency stems mainly from the basinwide decrease in the typhoon genesis, which is caused by the unfavorable dynamical environment as discussed previously.

Liu and Chan (2013) pointed out that the annual tropical cyclone genesis numbers over the WNP have experienced an inactive period during 1998–2011. Our results here indicate a significant drop in the late-season typhoon counts, which varies consistently with the annual tropical cyclone numbers. However, the activity of tropical cyclones during the early season (April–June) reveals an opposite feature; TC activity tends to be more vigorous in recent years. Intense typhoons over the WNP were observed more frequently in May dating back to the year 2000 (Tu et al. 2011). Associated with the advance in the SCS monsoon onset dates, the number of SCS tropical cyclones generated during the period from mid-April to mid-May in 1994–2008 is close to double compared to what was generated in 1979–93 (Kajikawa and Wang 2012). These results suggest that the typhoon season has begun to occur earlier in recent years. If the seasonal cycle of typhoons does exhibit such decadal variability, it would widely affect the extreme weather-related policies for a number of countries. We intend to examine detailed characteristics and mechanisms associated with this possible shift in the typhoon season in a future study.

Acknowledgments. Comments from three anonymous reviewers are much appreciated. This work was supported by the NSFC (Grant 41375100), Research Project

of Chinese Ministry of Education (213014A), and International Pacific Research Center. The model simulations were performed on the Earth Simulator. We thank May Izumi for technical editing.

REFERENCES

Adler, R. F., and Coauthors, 2003: The version 2 Global Precipitation Climatology Project (GPCP) monthly precipitation analysis (1979–present). *J. Hydrometeor.,* **4,** 1147–1167, doi:10.1175/1525-7541(2003)004<1147:TVGPCP>2.0.CO;2.

Bell, G. D., and Coauthors, 2000: Climate assessment for 1999. *Bull. Amer. Meteor. Soc.,* **81,** S1–S50, doi:10.1175/1520-0477(2000)81[s1:CAF]2.0.CO;2.

Bister, M., and K. A. Emanuel, 1998: Dissipative heating and hurricane intensity. *Meteor. Atmos. Phys.,* **65,** 233–240, doi:10.1007/BF01030791.

Burgman, R. J., A. C. Clement, C. M. Mitas, J. Chen, and K. Esslinger, 2008: Evidence for atmospheric variability over the Pacific on decadal timescales. *Geophys. Res. Lett.,* **35,** L01704, doi:10.1029/2007GL031830.

Camargo, S. J., K. A. Emanuel, and A. H. Sobel, 2007: Use of a genesis potential index to diagnose ENSO effects on tropical cyclone genesis. *J. Climate,* **20,** 4819–4834, doi:10.1175/JCLI4282.1.

Chan, J. C. L., 2006: Comment on ''Changes in tropical cyclone number, duration, and intensity in a warming environment.'' *Science,* **311,** 1713, doi:10.1126/science.1121522.

——, 2008: Decadal variations of intense typhoon occurrence in the western North Pacific. *Proc. Roy. Soc. London,* **464A,** 249–272, doi:10.1098/rspa.2007.0183.

——, 2009: Thermodynamic control on the climate of intense tropical cyclones. *Proc. Roy. Soc. London,* **465A,** 3011–3021, doi:10.1098/rspa.2009.0114.

Chang, C. P., P. A. Harr, and H.-J. Chen, 2005: Synoptic disturbances over the equatorial South China Sea and western maritime continent during boreal winter. *Mon. Wea. Rev.,* **133,** 489–503, doi:10.1175/MWR-2868.1.

Chikamoto, Y., M. Kimoto, M. Watanabe, M. Ishii, and T. Mochizuki, 2012: Relationship between the Pacific and Atlantic stepwise climate change during the 1990s. *Geophys. Res. Lett.,* **39,** L21710, doi:10.1029/2012GL053901.

Chu, P.-S., 2002: Large-scale circulation features associated with decadal variations of tropical cyclone activity over the central North Pacific. *J. Climate,* **15,** 2678–2689, doi:10.1175/1520-0442(2002)015<2678:LSCFAW>2.0.CO;2.

——, and X. Zhao, 2004: Bayesian change-point analysis of tropical cyclone activity: The central North Pacific case. *J. Climate,* **17,** 4893–4901, doi:10.1175/JCLI-3248.1.

——, and ——, 2011: Bayesian analysis for extreme climatic events: A review. *Atmos. Res.,* **102,** 243–262, doi:10.1016/j.atmosres.2011.07.001.

Du, Y., L. Yang, and S. P. Xie, 2011: Tropical Indian Ocean influence on northwest Pacific tropical cyclones in summer following strong El Niño. *J. Climate,* **24,** 315–322, doi:10.1175/2010JCLI3890.1.

Elsner, J. B., J. P. Kossin, and T. H. Jagger, 2008: The increasing intensity of the strongest tropical cyclones. *Nature,* **455,** 92–95, doi:10.1038/nature07234.

Emanuel, K. A., 1995: Sensitivity of tropical cyclones to surface exchange coefficients and a revised steady-state model incorporating eye dynamics. *J. Atmos. Sci.,* **52,** 3969–3976, doi:10.1175/1520-0469(1995)052<3969:SOTCTS>2.0.CO;2.

——, 2005: Increasing destructiveness of tropical cyclones over the past 30 years. *Nature,* **436,** 686–688, doi:10.1038/nature03906.

——, and D. S. Nolan, 2004: Tropical cyclone activity and global climate. Preprints, *26th Conf. on Hurricanes and Tropical Meteorology,* Miami, FL, Amer. Meteor. Soc., 240–241.

Gill, J., 2002: *Bayesian Methods: A Social and Behavioral Sciences Approach.* Chapman & Hall, 459 pp.

Goldenberg, S. B., C. W. Landsea, A. M. Mestas-Nunez, and W. M. Gray, 2001: The recent increase in Atlantic hurricane activity: Causes and implications. *Science,* **293,** 474–479, doi:10.1126/science.1060040.

Gray, W. M., 1979: Hurricanes: Their formation, structure and likely role in the tropical circulation. *Meteorology over the Tropical Oceans,* D. B. Shaw, Ed., Royal Meteorological Society, 155–218.

Harr, P. A., and J. C. L. Chan, 2005: Monsoon impacts on tropical cyclone variability. WMO Tech. Doc. 1266, 512–542.

Ho, C.-H., J.-J. Baik, J.-H. Kim, D.-Y. Gong, and C.-H. Sui, 2004: Interdecadal changes in summertime typhoon tracks. *J. Climate,* **17,** 1767–1776, doi:10.1175/1520-0442(2004)017<1767:ICISTT>2.0.CO;2.

Holland, G. J., and P. J. Webster, 2007: Heightened tropical cyclone activity in the North Atlantic: Natural variability or climate trend? *Philos. Trans. Roy. Soc.,* **A365,** 2695–2716, doi:10.1098/rsta.2007.2083.

Jin, C.-S., C.-H. Ho, J.-H. Kim, D.-K. Lee, D.-H. Cha, and S. W. Yeh, 2013: Critical role of northern off-equatorial sea surface temperature forcing associated with Central Pacific El Niño in more frequent tropical cyclone movement toward East Asia. *J. Climate,* **26,** 2534–2545, doi:10.1175/JCLI-D-12-00287.1.

JTWC, cited 2012: The Joint Typhoon Warning Center western North Pacific best track data. [Available online at http://www.usno.navy.mil/NOOC/nmfc-ph/RSS/jtwc/best_tracks/wpindex.html.]

Kajikawa, Y., and B. Wang, 2012: Interdecadal change of the South China Sea summer monsoon onset. *J. Climate,* **25,** 3207–3218, doi:10.1175/JCLI-D-11-00207.1.

Kamahori, H., N. Yamazaki, N. Mannoji, and K. Takahashi, 2006: Variability in intense tropical cyclone days in the western North Pacific. *SOLA,* **2,** 104–107, doi:10.2151/sola.2006-027.

Kendall, M. G., 1975: *Rank Correlation Methods.* Charles Griffin, 202 pp.

Knapp, K. R., M. C. Kruk, D. H. Levinson, H. J. Diamond, and C. J. Neumann, 2010: The International Best Track Archive for Climate Stewardship (IBTrACS): Unifying tropical cyclone data. *Bull. Amer. Meteor. Soc.,* **91,** 363–376, doi:10.1175/2009BAMS2755.1.

Kossin, J. P., K. R. Knapp, D. J. Vimont, R. J. Murnane, and B. A. Harper, 2007: A globally consistent reanalysis of hurricane variability and trends. *Geophys. Res. Lett.,* **34,** L04815, doi:10.1029/2006GL028836.

Landsea, C. W., 2005: Hurricanes and global warming. *Nature,* **438,** E11–E12, doi:10.1038/nature04477.

Lin, Y.-L., and C.-S. Lee, 2011: An analysis of tropical cyclone formations in the South China Sea during the late season. *Mon. Wea. Rev.,* **139,** 2748–2760, doi:10.1175/2011MWR3495.1.

Liu, K. S., and J. C. L. Chan, 2008: Interdecadal variability of western North Pacific tropical cyclone tracks. *J. Climate,* **21,** 4464–4476, doi:10.1175/2008JCLI2207.1.

——, and ——, 2013: Inactive period of western North Pacific tropical cyclone activity in 1998–2011. *J. Climate,* **26,** 2614–2630, doi:10.1175/JCLI-D-12-00053.1.

Mann, H. B., 1945: Non-parametric test against trend. *Econometrica,* **13,** 245–259, doi:10.2307/1907187.

——, and D. R. Whitney, 1947: On a test of whether one of two random variables is stochastically larger than the other. *Ann. Math. Stat.,* **18,** 50–60, doi:10.1214/aoms/1177730491.

Matsuura, T., M. Yumoto, and S. Iizuka, 2003: A mechanism of interdecadal variability of tropical cyclone activity over the western North Pacific. *Climate Dyn.,* **21,** 105–117, doi:10.1007/s00382-003-0327-3.

McBride, J. L., 1995: Tropical cyclone formation. *Global Perspectives on Tropical Cyclones,* R. L. Elsberry, Ed., World Meteorological Organization, 63–105.

Mizuta, R., and Coauthors, 2012: Climate simulations using the improved MRI-AGCM with 20-km grid. *J. Meteor. Soc. Japan,* **90A,** 233–258, doi:10.2151/jmsj.2012-A12.

Molinari, J., and D. Vollaro, 2013: What percentage of western North Pacific tropical cyclones form within the monsoon trough? *Mon. Wea. Rev.,* **141,** 499–505, doi:10.1175/MWR-D-12-00165.1.

Murakami, H., and B. Wang, 2010: Future change of North Atlantic tropical cyclone tracks: Projection by a 20-km-mesh global atmospheric model. *J. Climate,* **23,** 2699–2721, doi:10.1175/2010JCLI3338.1.

——, and Coauthors, 2012: Future changes in tropical cyclone activity projected by the new high-resolution MRI-AGCM. *J. Climate,* **25,** 3237–3260, doi:10.1175/JCLI-D-11-00415.1.

——, B. Wang, T. Li, A. Kitoh, 2013: Projected increase in tropical cyclones near Hawaii. *Nat. Climate Change,* **3,** 749–754, doi:10.1038/nclimate1890.

Rayner, N. A., D. E. Parker, E. B. Horton, C. K. Folland, L. V. Alexander, and D. P. Rowell, 2003: Global analysis of sea surface temperature, sea ice, and night marine air temperature since the late nineteenth century. *J. Geophys. Res.,* **108,** 4407, doi:10.1029/2002JD002670.

RSMC, cited 2012: Regional Specialized Meteorological Centers–Tokyo Typhoon Center tropical cyclone data. [Available online at http://www.jma.go.jp/jma/jma-eng/jma-center/rsmc-hp-pub-eg/trackarchives.html.]

Simiu, E., and R. H. Scanlon, 1978: *Wind Effects on Structures.* Wiley Interscience, 458 pp.

Simmons, A., S. Uppala, D. Dee, and S. Kobayashi, 2007: ERA-Interim: New ECMWF reanalysis products from 1989 onwards. *ECMWF Newsletter,* No. 110, ECMWF, Reading, United Kingdom, 25–35.

Takayabu, Y. N., and T. Nitta, 1993: 3–5 day disturbances coupled with convection in over the tropical Pacific Ocean. *J. Meteor. Soc. Japan,* **71,** 221–245.

Tu, J.-Y., C. Chou, and P.-S. Chu, 2009: The abrupt shift of typhoon activity in the vicinity of Taiwan and its association with western North Pacific–East Asian climate change. *J. Climate,* **22,** 3617–3628, doi:10.1175/2009JCLI2411.1.

——, ——, P. Huang, and R. Huang, 2011: An abrupt increase of intense typhoons over the western North Pacific in early summer. *Environ. Res. Lett.,* **6,** 034013, doi:10.1088/1748-9326/6/3/034013.

Wang, B., and J. C. L. Chan, 2002: How strong ENSO events affect tropical storm activity over the western North Pacific. *J. Climate,* **15,** 1643–1658, doi:10.1175/1520-0442(2002)015<1643:HSEEAT>2.0.CO;2.

Webster, P. J., G. J. Holland, J. A. Curry, and H.-R. Chang, 2005: Changes in tropical cyclone number, duration, and intensity in a warming environment. *Science,* **309,** 1844–1846, doi:10.1126/science.1116448.

Wilcoxon, F., 1945: Individual comparisons by ranking methods. *Biom. Bull.,* **1,** 80–83, doi:10.2307/3001968.

Wu, L., B. Wang, and S. Geng, 2005: Growing typhoon influence on East Asia. *Geophys. Res. Lett.,* **32,** L18703, doi:10.1029/2005GL022937.

Wu, M.-C., K.-H. Yeung, and W.-L. Chang, 2006: Trends in western North Pacific tropical cyclone intensity. *Eos, Trans. Amer. Geophys. Union,* **87,** 537–538, doi:10.1029/2006EO480001.

Yeh, S.-W., S.-K. Kang, B. P. Kirtman, J.-H. Kim, M.-H. Kwon, and C.-H. Kim, 2010: Decadal change in relationship between western North Pacific tropical cyclone frequency and the tropical Pacific SST. *Meteor. Atmos. Phys.,* **106,** 179–189, doi:10.1007/s00703-010-0057-0.

Yokoi, S., and Y. N. Takayabu, 2013: Attribution of decadal variability in tropical cyclone passage frequency over the western North Pacific: A new approach emphasizing the genesis place of cyclones. *J. Climate,* **26,** 973–987, doi:10.1175/JCLI-D-12-00060.1.

Zhan, R., Y. Wang, and C.-C. Wu, 2011: Impact of SSTA in the East Indian Ocean on the frequency of northwest Pacific tropical cyclones: A regional atmospheric model. *J. Climate,* **24,** 6227–6242, doi:10.1175/JCLI-D-10-05014.1.

Zhao, X., and P.-S. Chu, 2010: Bayesian changepoint analysis for extreme events (typhoons, heavy rainfall, and heat waves): An RJMCMC approach. *J. Climate,* **23,** 1034–1046, doi:10.1175/2009JCLI2597.1.